Biochemical and Biophysical Research Communications 456 (2015) 780–784

Contents lists available at ScienceDirect

Biochemical and Biophysical Research Communications

journal homepage: www.elsevier.com/locate/ybbrc

Crystal structure of the polo-box domain of polo-like kinase 2

Hong-Mei Shan [a], Tao Wang [b,*], Jun-Min Quan [a,*]

[a] Key Laboratory of Structural Biology, School of Chemical Biology & Biotechnology, Peking University Shenzhen Graduate School, Shenzhen 518055, China
[b] Laboratory for Computational Chemistry & Drug Design, School of Chemical Biology & Biotechnology, Peking University, Shenzhen Graduate School, Shenzhen 518055, China

ARTICLE INFO

Article history:
Received 22 November 2014
Available online 13 December 2014

Keywords:
Polo-like kinase 2
Polo-box domain
Cell cycle
DNA damage
Neuronal activity

ABSTRACT

Polo-like kinase 2 (PLK2) is a crucial regulator in cell cycle progression, DNA damage response, and neuronal activity. PLK2 is characterized by the conserved N-terminal kinase domain and the unique C-terminal polo-box domain (PBD). The PBD mediates diverse functions of PLK2 by binding phosphorylated Ser-pSer/pThr motifs of its substrates. Here, we report the first crystal structure of the PBD of PLK2. The overall structure of the PLK2 PBD is similar to that of the PLK1 PBD, which is composed by two polo boxes each contain β6α structures that form a 12-stranded β sandwich domain. The edge of the interface between the two polo boxes forms the phosphorylated Ser-pSer/pThr motifs binding cleft. On the hand, the peripheral regions around the core binding cleft of the PLK2 PBD is distinct from that of the PLK1 PBD, which might confer the substrate specificity of the PBDs of the polo-like kinase family.

1. Introduction

Polo-like kinases (PLKs) are key players in multiple biological processes including cell cycle progression, DNA replication and DNA damage response, cilia disassembly, centriole biogenesis and duplication, and neuronal activity [1–6]. Currently five mammalian PLK family members, PLK1–5, have been identified [7]. Despite their distinct biological functions, all the five PLK family members are characterized by an N-terminal kinase domain and a C-terminal polo-box domain (PBD). The kinase domain is highly similar to the kinase domains of other serine–threonine protein kinases, while the PBD is unique to the PLK family [8], which regulates the kinase activity, subcellular localization, and substrate interactions through binding the phosphorylated Ser-pSer/pThr motifs of its target proteins [9,10]. The PBD of PLK1 (PBD1) has been extensively studied and characterized based on the determined structures of the PBD in complex with the phosphopeptides [10–12] or in complex with the kinase domain of PLK1 [13], but much less is known about the PBDs of other members than about that of PLK1 [14].

Among the five members, PLK2 is the more closely related to PLK1, which has been shown to play crucial roles in the nervous system such as synaptic regulation [15] and neuronal protection [16]. PLK2 regulates synaptic plasticity by mediating degradation of SPAR (spine-associated RapGAP) via ubiquitin–proteasome pathway, and might protect neuron by mediating degradation of α-synuclein via lysosome-autophagy pathway. Both neuronal functions of PLK2 depend on its C-terminal PBD to bind the phosphorylated substrates and lead to their degradation [15,16]. The PBD of PLK2 (PBD2) bind phosphorylated Ser-pSer/pThr motifs as the closely related PLK1 but with much lower affinity [17]. However, the understanding of the molecular basis for the substrate specificity of the PBDs has been hindered by the lack of the crystal structure of the PBD of PLK2. To address this problem, we determined the crystal structure of the PBD of PLK2 at 2.6 Å resolution, which provide structural insight into understand the substrate specificity of the PBDs of PLKs.

2. Materials and methods

2.1. Protein expression and purification

The DNA fragment of human PLK2 (residues 451–685) was amplified by PCR and cloned into the *EcoRI* and *XhoI* sites of expression vector pGEX-6p-1 or pGEX-6p-2. Proteins were expressed in BL21 (DE3) pLysS strains. Point mutations were introduced using Easy mutagenesis system (TransGen Biotech). Cells were grown to an optical density of 0.6 at 37 °C with vigorous shaking and then cooled to 25 °C, induced by a final concentration 0.1 mM IPTG. The cells were harvested and frozen at −80 °C. The cells were thawed in buffer A (20 mM Tris, 500 mM NaCl, 1 mM DTT pH = 8.0) and lysed by addition of 0.1 mg/ml DNase I (sigma), $MgCl_2$, 1 mg/ml Lysozyme (sigma) and 0.1% Triton X-100 [18]. The lysate was centrifuged at 13000*g* for 30 min and the supernatant was filtered

* Corresponding authors.
E-mail addresses: tau@pku.edu.cn (T. Wang), quanjm@pkusz.edu.cn (J.-M. Quan).

http://dx.doi.org/10.1016/j.bbrc.2014.11.125
0006-291X/

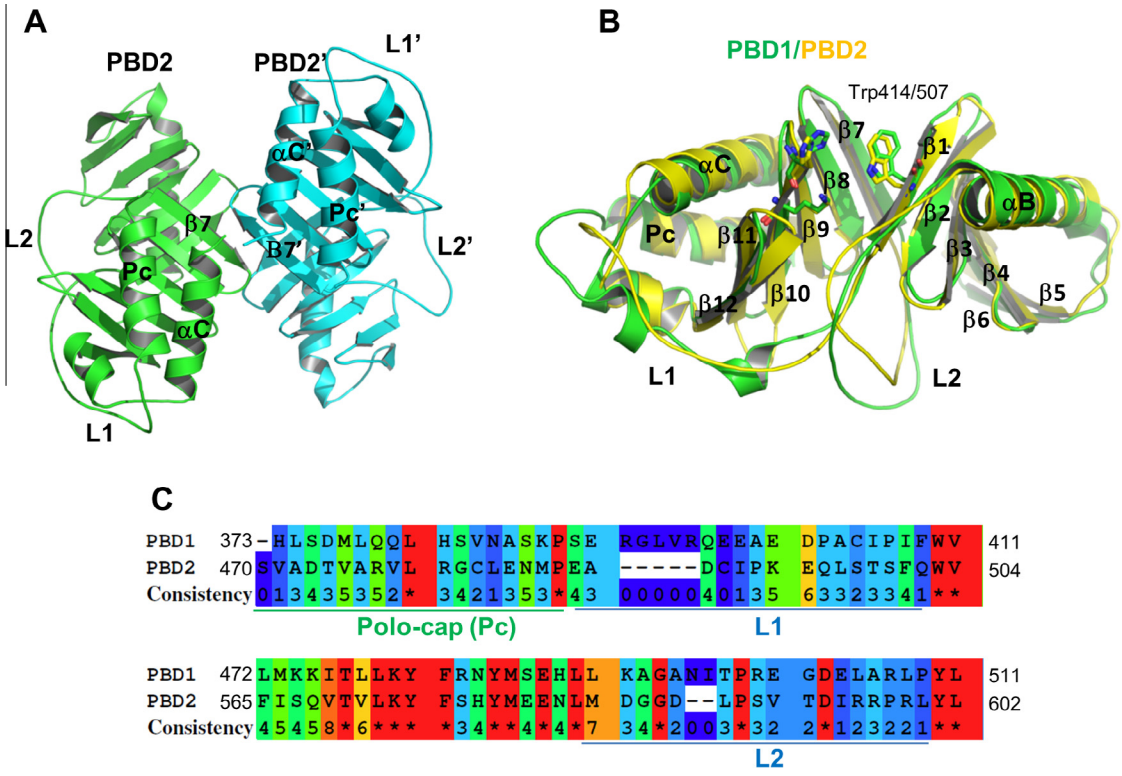

Fig. 1. Overall structure of PBD2. (A) The dimeric structure of PBD2 in one asymmetric unit. (B) Superposition of the structures of PBD1 (green) (PDB code 1UMW) [10] and PBD2 (yellow). (C) Sequence alignment of the Polo-cap, L1, and L2 regions of PBD1 and PBD2. (For interpretation of the references to colour in this figure legend, the reader is referred to the web version of this article.)

through 0.45 μm filter. The supernatant was loaded into glutathione–Sepharose column (GE Healthcare), washed with buffer A and eluted with 20 mM glutathione in buffer A. The GST tag was digested with 3C precision protease overnight. The digestion was reloaded onto glutathione–Sepharose column. The flowthrough was collected and concentrated and then loaded onto a gel-filtration column (Superdex200, GE Healthcare). The protein was concentrated into 9 mg/ml and stored at −80 °C.

2.2. Crystallization and structure determination

Initially crystal screening was performed using sitting-drop method. Small crystals were obtained overnight using Index and Crystal Screens (Hampton Research, CA, USA). Crystals were grown at 20 °C in hanging drops using Index 28 containing 35% v/v Tacsimate TM pH 7.0. The initial diffraction data was collected at beamline BL17U of the Shanghai Synchrotron Radiation facility (λ = 0.9793 Å) at 100 K. The crystal structure of PBD2 451–685 was determined by molecular replacement using Phaser-PHENIX [19,20] suite based on the crystal structure of PBD1 (PDB code 1UMW) [10] encompassing residues 373–595. The refinement of the initial solutions with manually built in Coot [21] and refined by Refmac [22] in CCP4 [23] yielded experimental electron-density map for model building. The final atomic model of the PBD2 was refined to an R factor of 0.186 and an R_{free} value of 0.247 at 2.6 Å resolution. The protein in the figures was rendered with PyMol [24].

2.3. Fluorescence polarization assay

Binding assays were carried out essentially as described previously [25]. In brief, FITC-labeled phospho-peptide FITC-GPMQTSpTPKNG (10 nM) (GL Biochem Shanghai Ltd) was titrated by the PBD of PLK2 in a buffer containing 20 mM Tris, and 200 mM NaCl, pH 8.0. All the experiments were performed in 96-well black plates using Envision multilabel reader (Perkin Elmer). Plates were read one hour after mixing of all assay components.

3. Results and discussion

3.1. Overall structure of the polo-box domain$_{451–685}$

According to the sequence alignment between PBD1 and PBD2, PBD2 containing residues 451–685 was constructed, purified and crystallized. The crystal structure was determined by molecular replacement using the crystal structure of the PBD1 (PDB code 1UMW) [10] as the template, which was solved at 2.6 Å in the I23 space group with a dimer in the asymmetric unit (Fig. 1A and Table 1). The structure of PBD2 contains residues 470–682, residues at the two extreme terminuses were not observed in the solved crystal structure.

The overall structure of PBD2 resembles the structure of PBD1 (Fig. 1B), composed of two tandem polo boxes (PB1 and PB2) that have identical β6α fold. The N-terminal extension (residues 470–486) forms the helical Polo-cap (Pc) that wraps around PB2 and connects to PB1 via a linker region (residues 487–502, or L1), while PB1 and PB2 are connected by a secondary linker region (residues 584–600, or L2). Structural superposition reveals an RMSD of 0.99 Å for 152 equivalent α-carbons between PBD2 and PBD1 despite their low sequence identity (about 32%). The major structural variations locate at the two linker regions L1 and L2, which is consistent with the low sequence homology in these regions between PBD2 and PBD1 (Fig. 1C).

3.2. The conservation of the phosphopeptide binding cleft

Both PBD2 and PBD1 bind phosphopeptides containing a Ser-pSer/pThr motif, but PBD2 binds such peptides with lower binding

Table 1
Data collection and refinement statistics (molecular replacement).

PBD ID	4RS6
Data collection	
Wavelength (Å)	0.9792
Space group	I23
Cell dimensions	
a, *b*, *c* (Å)	153.08, 153.08, 153.08
α, β, γ (°)	90, 90, 90
Resolution (Å)	2.60(2.64–2.60)*
Total reflections	407752
R_{sym}	0.15(0.866)*
$I/\sigma I$	27.56(6.0)*
Completeness (%)	99.98(100.0)*
Redundancy	22.1(22.6)*
Refinement	
Resolution (Å)	25.0–2.60
Unique reflections	18474
R_{work}/R_{free}	0.186/0.247
No. atoms	3462
Protein	3448
Ligand/ion	
Water	14
Average B factors	72.5
r.m.s. deviations	
Bond lengths (Å)	0.015
Bond angles (°)	1.730
Ramachandran statistics	
Most favored (%)	93.0
Allowed (%)	6.53
Outlier (%)	0.47

Equations defining various *R* values are standard and hence are no longer defined in the footnotes.
Important notice: diffraction is completely lost in the edge of 2.6 Å.
* Values in parentheses are for highest-resolution shell.

affinity [17]. The crystal structures of PBD2 and PBD1 provide a framework for understanding the molecular basis underlying the substrate specificity.

The PBDs recognize the phosphorylated Ser-pSer/pThr motif by a highly conserved cleft located at the edge of the interface between the two polo boxes. Previous structural and biochemical data [10–12] have shown that a core region containing three conserved residues (Trp414, H538, and Lys540) of PBD1 are essential for the binding with the phosphorylated Ser-pSer/pThr motif, in which Trp414 engages in hydrogen bonding and hydrophobic interactions with Ser-1 of the Ser-pSer/pThr motif, and the pincer residues H538/Lys540 form electrostatic interactions with the phosphate group of the Ser-pSer/pThr motif (Fig. 2A). We failed to crystallize the complex of PBD2 with the phosphopeptide, but structural analysis reveals that the core region of the binding clef in the apo PBD2 is highly similar to that of PBD1 in complex with the phosphopeptide. Mutation of any the three corresponding conserved residues (W507F, H629A, and K631M) eliminates the capability of PBD2 binding with the phosphopeptide (Fig. 2B), indicating that the phosphopeptide would bind with PBD2 in a similar mode to that of binding with PBD1.

Unlike the high conservation of the core region of the phosphopeptide binding cleft, the residues in the peripheral regions around the core region involved in the binding are relatively divergent between PBD2 and PBD1 (Fig. 3). One divergent region locates at β7 and β9 of the PBDs that is the site for binding the N-terminus of the phosphopeptide, and another divergent region locates at the linker region L2 that is important to bind with the C-terminus of the phosphopeptide. These distinct regions might confer the substrate specificity.

Arg516 on β7 and Phe535 on β9 in PBD1 are two key residues involved in binding with the phosphopeptide, while the corresponding residues in PBD2 are Lys607 and Tyr626, respectively (Fig. 3A). Arg516 in PBD1 forms favorable electrostatic interactions with the carbonyl oxygen of the N-terminus of the phosphopeptide, but more flexible Lys607 in PBD2 might weaken such interactions. In addition, Phe535 and Trp414 in PBD1 forms hydrophobic pocket to accommodate the hydrophobic residue on the N-terminus of the phosphopeptide, but more polar Tyr626 partially impair the hydrophobic packing with Trp507 in PBD2. L2 is another key region for binding with the phosphopeptide by the backbone hydrogen bonding and side-chain hydrophobic interaction. L2 forms extensive hydrogen bonding network with β1/2/3 in PBD1 (Fig. 3B), but L2 just forms a single hydrogen bond with β1 in PBD2 (Fig. 3C). L2 of PBD1 is thus more rigid and favorable for binding with the phosphopeptide.

3.3. Crystal packing of the polo-box domain in the lattice

The crystal structure of PBD2 was solved as a dimer in one asymmetric unit (Figs. 1A and 4A), but the purified PBD2 (residues 451–685) was a monomer in solution as reflected by a single peak during gel filtration corresponding to apparent molecular mass of

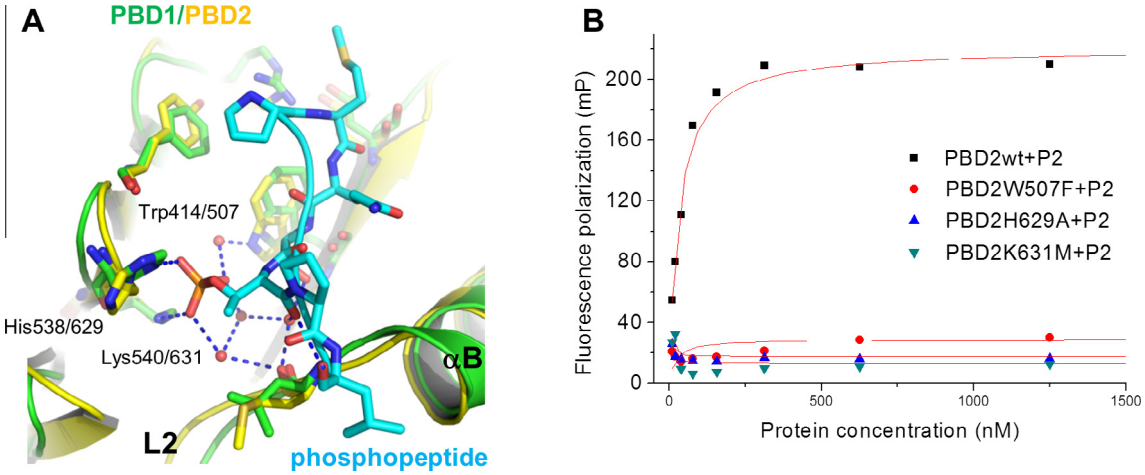

Fig. 2. Interactions between the phosphopeptide with the PBDs. (A) Superposition of the structure of apo PBD2 (yellow) with the structure of the complex of PBD1 (green) with the phosphopeptide (cyan) (PDB code 1UMW) [10]. The three conserved residues in the core region are labeled and numbered according to their sequences. (B) The binding of the FITC-labeled phospho-peptide FITC-GPMQTSpTPKNG (P2) with PBD2 and its mutants by fluorescence polarization assay. (For interpretation of the references to colour in this figure legend, the reader is referred to the web version of this article.)

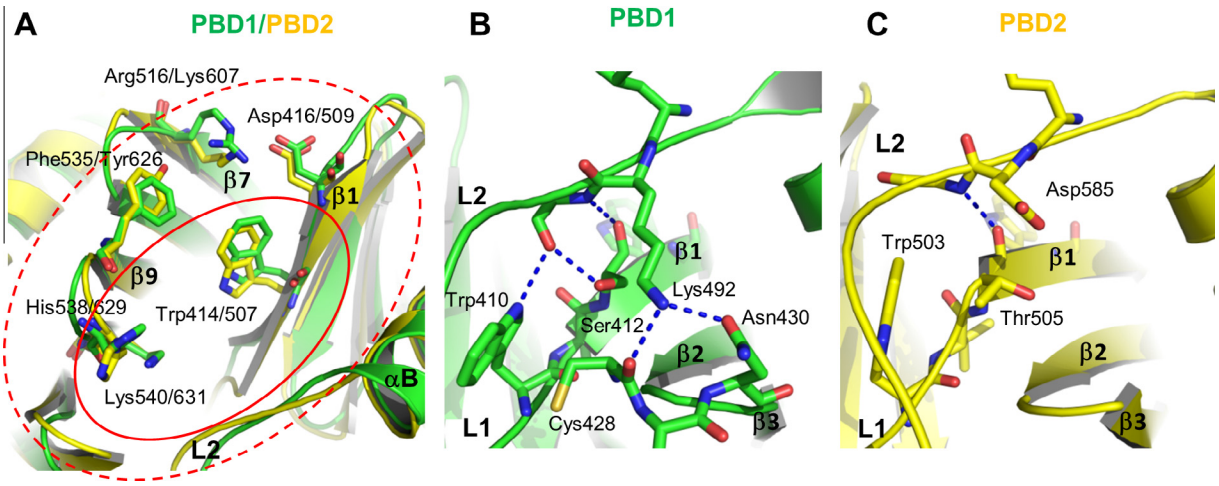

Fig. 3. Comparison of the peripheral regions of the phosphopeptide binding cleft of PBD1 and PBD2. (A) The core and peripheral regions of the phosphopeptide binding cleft in PBD1 and PBD2. The core region is labeled by red solid line ellipse, and the peripheral region is labeled by red dash line ellipse. (B) Hydrogen bonding network formed by L2 region in PBD1. Hydrogen bonds are indicated by blue dashed lines in all figures. (C) Hydrogen bond formed by L2 region in PBD2. (For interpretation of the references to colour in this figure legend, the reader is referred to the web version of this article.)

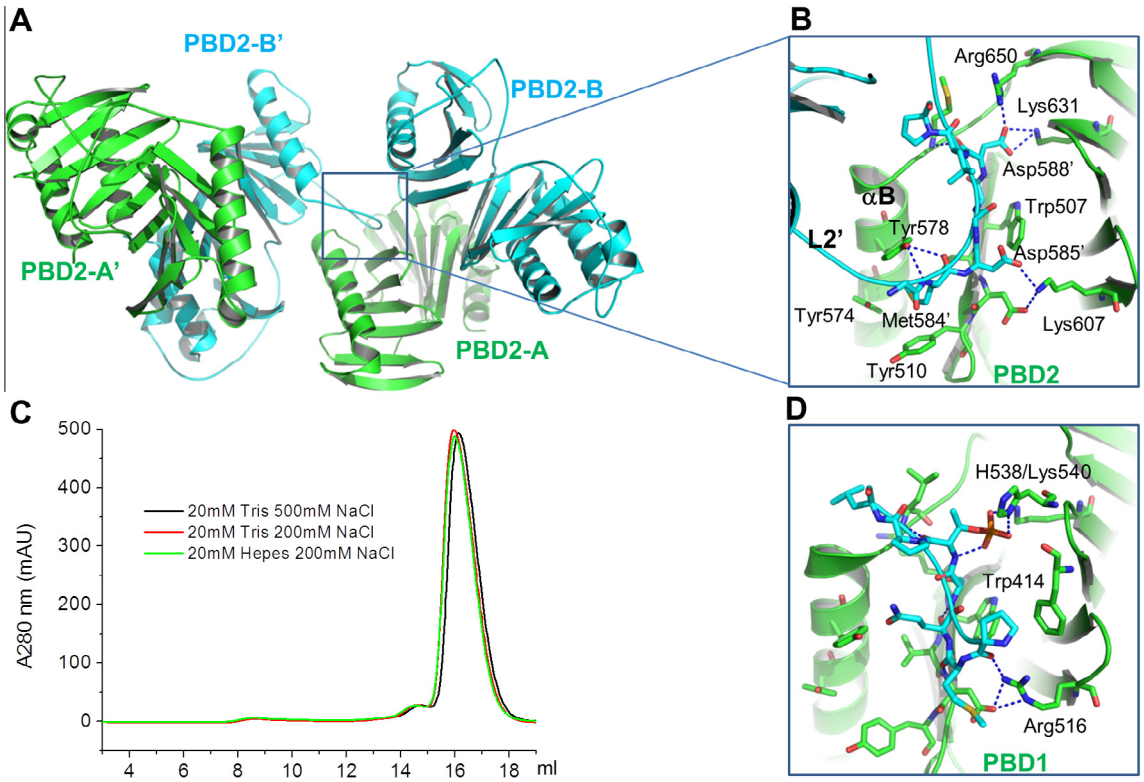

Fig. 4. Crystal packing of PBD2 in the crystal lattice. (A) Structures of PBD2 in two neighboring asymmetric units, each asymmetric unit contains a dimer of PBD2. (B) The packing of L2' of PBD2 with the phosphopeptide binding cleft of PBD2 in the neighboring asymmetric units. Hydrogen bonds are indicated by blue dashed lines. (C) Size exclusion profile of purified PBD2 in different salt conditions. (D) Structure of the complex of PBD1 with the phosphopeptide (PDB code 1UMW) [10]. (For interpretation of the references to colour in this figure legend, the reader is referred to the web version of this article.)

about 26 kDa (Fig. 4C). The dimeric state in the crystal thus might be caused by the crystal packing in the high protein concentration. Interestingly, detailed analysis of the crystal packing in the crystal lattice revealed that the phosphopeptide binding cleft of PBD2 was occupied the linker region L2' of PBD2 from the neighboring asymmetric unit (Fig. 4A). The binding mode of L2' in the binding cleft of PBD2 is highly similar to that of the phosphopeptide in PBD1 (Fig. 4B and D). Asp588' of L2' mimics the phosphate group of the Ser-pSer/pThr motif to form electrostatic interacts with Lys631 and Arg650, and Asp585' of L2' mimics the carbonyl oxygen of the N-terminus of the phosphopeptide to form additional electrostatic interaction with Lys607. In addition, Met584' of L2' perfectly docks into the cryptic hydrophobic pocket formed by Tyr510, Tyr574, and Tyr578 [26,27]. This phosphopeptide-like

packing in the crystal might explain the reason why we cannot crystallize the complex of PBD2 with the phosphopeptide because the binding phosphopeptide would disrupt the crystal packing.

Acknowledgments

This work was supported by funds from the Ministry of Science and Technology 2012CB722602 (to J.M.Q.), 2013CB911501 (to T.W.); the NSFC21290183 (to J.M.Q.), NSFC31300600 (to T.W.); Shenzhen government JCYJ20130331144947526 and GJHZ20120614144733420 (to J.M.Q.), ZDSY20120614 144410389 and JCYJ20120614150904060 (to T.W). We thank the staff of beamline BL17U at Shanghai Synchrotron Radiation Facility for the technical assistance during data collection.

References

[1] M. Petronczki, P. Lenart, J.M. Peters, Polo on the rise-from mitotic entry to cytokinesis with plk1, Dev. Cell 14 (2008) 646–659.
[2] V. Archambault, D.M. Glover, Polo-like kinases: conservation and divergence in their functions and regulation, Nat. Rev. Mol. Cell Biol. 10 (2009) 265–275.
[3] K. Strebhardt, Multifaceted polo-like kinases: drug targets and antitargets for cancer therapy, Nat. Rev. Drug Discov. 9 (2010) 643–660.
[4] S. Zitouni, C. Nabais, S.C. Jana, A. Guerrero, M. Bettencourt-Dias, Polo-like kinases: structural variations lead to multiple functions, Nat. Rev. Mol. Cell Biol. 15 (2014) 433–452.
[5] F.A. Barr, H.H. Sillje, E.A. Nigg, Polo-like kinases and the orchestration of cell division, Nat. Rev. Mol. Cell Biol. 5 (2004) 429–440.
[6] D.P. Seeburg, D. Pak, M. Sheng, Polo-like kinases in the nervous system, Oncogene 24 (2005) 292–298.
[7] G. de Cárcer, G. Manning, M. Malumbres, From Plk1 to Plk5: functional evolution of polo-like kinases, Cell Cycle 10 (2011) 2255–2262.
[8] J.E. Park, N.K. Soung, Y. Johmura, Y.H. Kang, C. Liao, K.H. Lee, C.H. Park, M.C. Nicklaus, K.S. Lee, Polo-box domain: a versatile mediator of polo-like kinase function, Cell. Mol. Life Sci. 67 (2010) 1957–1970.
[9] A.E. Elia, L.C. Cantley, M.B. Yaffe, Proteomic screen finds pSer/pThr-binding domain localizing Plk1 to mitotic substrates, Science 299 (2003) 1228–1231.
[10] A.E.H. Elia, P. Rellos, L.F. Haire, J.W. Chao, F.J. Ivins, K. Hoepker, D. Mohammad, L.C. Cantley, S.J. Smerdon, M.B. Yaffe, The molecular basis for phosphodependent substrate targeting and regulation of plks by the polo-box domain, Cell 115 (2003) 83–95.
[11] K.Y. Cheng, E.D. Lowe, J. Sinclair, E.A. Nigg, L.N. Johnson, The crystal structure of the human polo-like kinase-1 polo box domain and its phospho-peptide complex, EMBO J. 22 (2003) 5757–5768.
[12] S.M. Yun, T. Moulaei, D. Lim, J.K. Bang, J.E. Park, S.R. Shenoy, F. Liu, Y.H. Kang, C. Liao, N.K. Soung, S. Lee, D.Y. Yoon, Y. Lim, D.H. Lee, A. Otaka, E. Appella, J.B. McMahon, M.C. Nicklaus, T.R. Burke Jr., M.B. Yaffe, A. Wlodawer, K.S. Lee, Structural and functional analyses of minimal phosphopeptides targeting the polo-box domain of polo-like kinase 1, Nat. Struct. Mol. Biol. 16 (2009) 876–882.
[13] J. Xu, C. Shen, T. Wang, J. Quan, Structural basis for the inhibition of Polo-like kinase 1, Nat. Struct. Mol. Biol. 20 (2013) 1047–1053.
[14] G.C. Leung, J.W. Hudson, A. Kozarova, A. Davidson, J.W. Dennis, F. Sicheri, The Sak polo-box comprises a structural domain sufficient for mitotic subcellular localization, Nat. Struct. Biol. 9 (2002) 719–724.
[15] D.P. Seeburg, M. Feliu-Mojer, J. Gaiottino, D.T. Pak, M. Sheng, Critical role of CDK5 and Polo-like kinase 2 in homeostatic synaptic plasticity during elevated activity, Neuron 58 (2008) 571–583.
[16] A. Oueslati, B.L. Schneider, P. Aebischer, H.A. Lashuel, Polo-like kinase 2 regulates selective autophagic alpha-synuclein clearance and suppresses its toxicity in vivo, Proc. Natl. Acad. Sci. U.S.A. 110 (2013) E3945–E3954.
[17] B.C. van de Weerdt, D.R. Littler, R. Klompmaker, A. Huseinovic, A. Fish, A. Perrakis, R.H. Medema, Polo-box domains confer target specificity to the Polo-like kinase family, Biochim. Biophys. Acta 1783 (2008) 1015–1022.
[18] B. Garcia-Alvarez, S. Ibanez, G. Montoya, Crystallization and preliminary X-ray diffraction studies on the human Plk1 Polo-box domain in complex with an unphosphorylated and a phosphorylated target peptide from Cdc25C, Acta Crystallogr. Sect. F Struct. Biol. Cryst. Commun. 62 (2006) 372–375.
[19] A.J. McCoy, R.W. Grosse-Kunstleve, P.D. Adams, M.D. Winn, L.C. Storoni, R.J. Read, Phaser crystallographic software, J. Appl. Crystallogr. 40 (2007) 658–674.
[20] P.D. Adams, P.V. Afonine, G. Bunkoczi, V.B. Chen, I.W. Davis, N. Echols, J.J. Headd, L.W. Hung, G.J. Kapral, R.W. Grosse-Kunstleve, A.J. McCoy, N.W. Moriarty, R. Oeffner, R.J. Read, D.C. Richardson, J.S. Richardson, T.C. Terwilliger, P.H. Zwart, PHENIX: a comprehensive python-based system for macromolecular structure solution, Acta Crystallogr. D Biol. Crystallogr. 66 (2010) 213–221.
[21] P. Emsley, K. Cowtan, Coot: model-building tools for molecular graphics, Acta Crystallogr. D Biol. Crystallogr. 60 (2004) 2126–2132.
[22] G.N. Murshudov, A.A. Vagin, E.J. Dodson, Refinement of macromolecular structures by the maximum-likelihood method, Acta Crystallogr. D Biol. Crystallogr. 53 (1997) 240–255.
[23] M.D. Winn, C.C. Ballard, K.D. Cowtan, E.J. Dodson, P. Emsley, P.R. Evans, R.M. Keegan, E.B. Krissinel, A.G. Leslie, A. McCoy, S.J. McNicholas, G.N. Murshudov, N.S. Pannu, E.A. Potterton, H.R. Powell, R.J. Read, A. Vagin, K.S. Wilson, Overview of the CCP4 suite and current developments, Acta Crystallogr. D Biol. Crystallogr. 67 (2011) 235–242.
[24] W.L. Delano, The PyMol Molecular Graphics System, Delano Scientific LLC, San Carlos, CA, USA, <http://www.pymol.org/>.
[25] W. Reindl, M. Graber, K. Strebhardt, T. Berg, Development of high-throughput assays based on fluorescence polarization for inhibitors of the polo-box domains of polo-like kinases 2 and 3, Anal. Biochem. 395 (2009) 189–194.
[26] F. Liu, J.E. Park, W.J. Qian, D. Lim, M. Gräber, T. Berg, M.B. Yaffe, K.S. Lee, T.R. Burke Jr., Serendipitous alkylation of a Plk1 ligand uncovers a new binding channel, Nat. Chem. Biol. 7 (2011) 595–601.
[27] P. Śledź, C.J. Stubbs, S. Lang, Y.Q. Yang, G.J. McKenzie, A.R. Venkitaraman, M. Hyvönen, C. Abell, From crystal packing to molecular recognition: prediction and discovery of a binding site on the surface of polo-like kinase 1, Angew. Chem. Int. Ed. Engl. 50 (2011) 4003–4006.